Simulation of noise-assisted transport via optical cavity networks

Filippo Caruso,[1,*] Nicolò Spagnolo,[2,3] Chiara Vitelli,[2,3] Fabio Sciarrino,[2,4,†] and Martin B. Plenio[1]

[1]*Institut für Theoretische Physik, Universität Ulm, DE-89069 Ulm, Germany*

[2]*Dipartimento di Fisica, Sapienza Università di Roma, IT-00185 Roma, Italy*

[3]*Consorzio Nazionale Interuniversitario per le Scienze Fisiche della Materia, IT-00185 Roma, Italy*

[4]*Istituto Nazionale di Ottica, IT-50125 Firenze, Italy*

(Received 19 August 2010; published 11 January 2011)

Recently, the presence of noise has been found to play a key role in assisting the transport of energy and information in complex quantum networks and even in biomolecular systems. Here we propose an experimentally realizable optical network scheme for the demonstration of the basic mechanisms underlying noise-assisted transport. The proposed system consists of a network of coupled quantum-optical cavities, injected with a single photon, whose transmission efficiency can be measured. Introducing dephasing in the photon path, this system exhibits a characteristic enhancement of the transport efficiency that can be observed with presently available technology.

DOI: 10.1103/PhysRevA.83.013811 PACS number(s): 37.30.+i, 42.79.Gn, 42.50.Ex, 03.65.Yz

I. INTRODUCTION

The presence of noise in quantum transmission networks is generally considered to be deleterious for the efficient transfer of energy or classical or quantum information encoded in quantum states. Quantum networks, used for the transmission, are unavoidably interacting with an external noisy environment, and this interaction significantly affects the quantum coherence of the system evolution. It is indeed commonly accepted that the presence of decoherence [1] is responsible for the undesired and uncontrolled transfer of information from the system to the environment, which in turn reduces the coherence in quantum systems. However, recently noise has been found to play a positive role in creating quantum coherence and entanglement [2,3]. Motivated by fascinating experiments showing the presence of quantum beating in photosynthetic systems [4–6], subsequent theoretical work pointed to the idea that the remarkable efficiency of the excitation energy transfer in light-harvesting complexes during photosynthesis benefits from the presence of environmental noise [7,8]. Indeed, the intricate interplay between dephasing and quantum coherence as well as the entanglement behavior during the noise-assisted transport dynamics have been elucidated in more detail in Refs. [9–12]. Perhaps even more surprisingly, the dephasing was recently found to assist the transfer of classical and quantum information in communication complex quantum networks [13].

Recently, quantum optical systems have been exploited as a promising platform to simulate quantum processes [14–16]. For example, several implementations of systems simulating quantum random walks have been reported with linear optical resonators [17,18], linear optical elements [19,20], fiber networks [21], and optical waveguides [22–25]. Motivated by these results, here we propose a quantum optical scheme to investigate the noise-assisted excitation transfer process through a set of coupled optical cavities. We discuss a four-site optical network and derive the set of relevant parameters that rule the time evolution of the system. A detailed numerical simulation of this dynamics, when one cavity is injected with a single photon, is performed employing realistic experimental parameters, showing that the presence of a suitable dephasing process in each site of the network allows for a characteristic increase of the excitation transfer efficiency. Furthermore, we consider aspects such as phase stabilization of the cavities and the implementation of dephasing, which are necessary to observe a clear enhancement of the photon transfer rate from one cavity to an external detector, mimicking the so-called reaction center of the light-harvesting complexes. Finally, we investigate how entanglement degrades during the time evolution of the optical network.

The paper is organized as follows: In Sec. II we define the model that describes the dynamics of the four-site optical network analyzed in this paper, including the master equation for the two relevant noise processes. Then in Sec. III we perform a detailed derivation of a realistic set of parameters for the system. In Sec. IV we report the results of a numerical simulation of the dynamics of the network. Finally, the conclusions and final remarks are presented in Sec. V.

II. MODEL OF THE NETWORK

In this section we describe in detail the model underlying the dynamics of the proposed network of optical cavities. A schematic view of this system in relation to the light-harvesting complexes is shown in Fig. 1. Starting from the Hamiltonian describing noninteracting cavities, one has

$$\hat{\mathcal{H}}_{\rm cav} = \sum_i \hbar\omega \hat{a}_i^\dagger \hat{a}_i, \tag{1}$$

where $\hat{a}_i$ and $\hat{a}_i^\dagger$ are the usual bosonic field operators, which annihilate and create a photon in cavity i, and ω is the resonance frequency, which we assume for simplicity to be equal for all cavities. The transfer of photons between the optical cavities is described by the following Hamiltonian term:

$$\hat{\mathcal{H}}_{\rm int} = \sum_{(i,j)} \hbar g_{ij} (\hat{a}_i^\dagger \hat{a}_j + \hat{a}_i \hat{a}_j^\dagger), \tag{2}$$

*filippo.caruso@uni-ulm.de

†fabio.sciarrino@uniroma1.it

 ©2011 American Physical Society

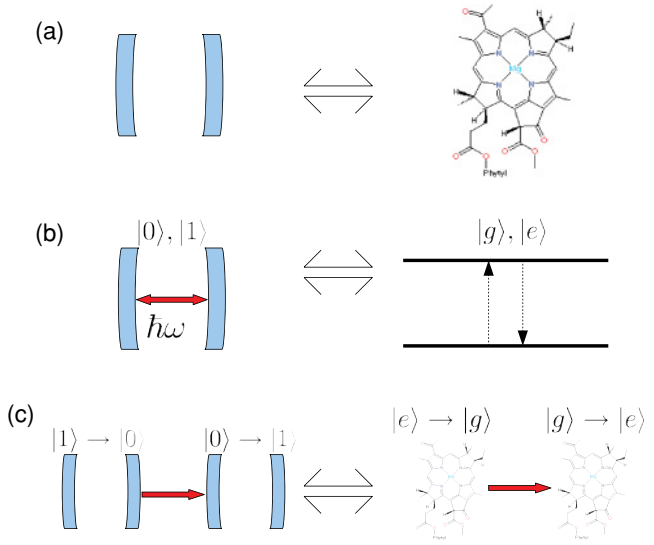

FIG. 1. (Color online) Analogy between a network of coupled optical cavities and a physical network where the excitation is carried by electrons, such as light-harvesting complexes. (a) The single site of the network is analogous to a single optical cavity. (b) The electronic excitation is represented by the presence of a single photon in the corresponding optical cavity. (c) The transfer of the excitation between two interacting sites is analogous to the transfer of the single-photon between two adjacent coupled cavities.

where the sum on (i, j) extends over all the connected cavities, and g_{ij} are the coupling constants. Moreover, we assume that this dynamics is subject simultaneously to two distinct noise processes acting on each optical cavity i:

(1) a dissipation process that leads to photon loss with rate Γ_i, described by the following Lindblad superoperator:

$$\mathcal{L}_{\rm diss}(\hat{\rho}) = \sum_i \Gamma_i(-\{\hat{a}_i^\dagger \hat{a}_i, \hat{\rho}\} + 2\hat{a}_i \hat{\rho} \hat{a}_i^\dagger), \tag{3}$$

(2) a pure dephasing process that randomizes the photon phase with rate γ_i given by a Lindbladian term which has the form

$$\mathcal{L}_{\rm deph}(\hat{\rho}) = \sum_i \gamma_i(-\{\hat{a}_i^\dagger \hat{a}_i \hat{a}_i^\dagger \hat{a}_i, \hat{\rho}\} + 2\hat{a}_i^\dagger \hat{a}_i \hat{\rho} \hat{a}_i^\dagger \hat{a}_i). \tag{4}$$

In addition, the total transfer of the single photon is measured in terms of photons detected on the right-hand side output of cavity 2, which represents the so-called sink or reaction center of the biological systems (here, a single-photon detector), described by the Lindblad operator

$$\mathcal{L}_{\rm det}(\rho) = \Gamma_{\rm det}[2\hat{a}_{\rm det}^\dagger \hat{a}_2 \rho \hat{a}_2^\dagger \hat{a}_{\rm det} - \{\hat{a}_2^\dagger \hat{a}_{\rm det} \hat{a}_{\rm det}^\dagger \hat{a}_2, \rho\}], \tag{5}$$

where $\hat{a}_{\rm det}^\dagger$ describes the effective photon creation operator in the detector and $\Gamma_{\rm det}$ is the rate at which the photon irreversibly gets the detector on the right side of optical cavity 2; see Figs. 2, 3, and 4. Hence, the photon transfer efficiency is measured by the quantity

$$p_{\rm sink}(t) = 2\Gamma_{\rm det} \int_0^t {\rm Tr}[\rho(t')\hat{a}_2^\dagger \hat{a}_2]\, dt'. \tag{6}$$

In the following numerical simulation, we will assume that there is a single photon initially in cavity 1. Notice that, since our scheme does not involve any nonlinear process, a single-photon experiment repeated many times exhibits the same statistics obtained with an injected coherent state [26].

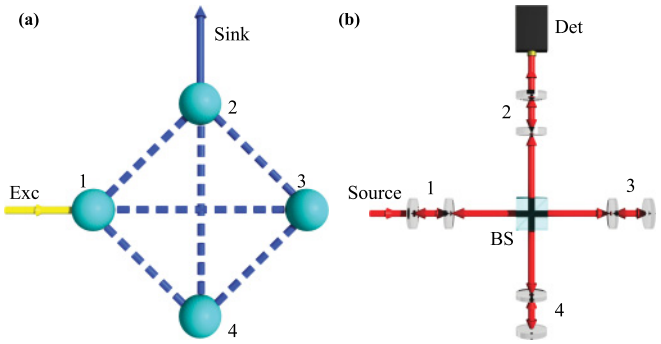

FIG. 2. (Color online) Quantum simulation of noise-assisted excitation transfer through a network of coupled optical cavities. (a) Simplified scheme of a four-site fully connected network. The excitation is injected at site 1, and exits from the network by coupling of site 2 with the output sink. (b) Equivalent network of four coupled cavities. The excitation is given by a single-photon pulse injected into cavity 1. The right output mode of cavity 2 is the output sink channel for the excitation.

III. PARAMETERS OF THE NETWORK

In this section we discuss the experimental details of the optical cavity network setup sketched in Fig. 2, in order to simulate the mechanisms underlying the noise-assisted transport phenomena. The excitation of the network, i.e., a single photon at wavelength $\lambda = 800$ nm, is generated through a heralded single-photon source, based on the spontaneous parametric down-conversion process. We consider the case of a network of $d_k = 1$ cm long cavities. The distance between each cavity and the central beam-splitter (BS), chosen with transmittivity $\eta = 0.5$, is taken to be $l_k = 20$ cm. More specifically, cavity 1 has mirror reflectivities $R_1^{\rm in} = 0.9$ (for the internal mirror pointing toward the BS) and $R_1^{\rm out} = 0.99$ (for the external mirror), cavity 2 has $R_2^{\rm in} = R_2^{\rm out} = 0.9$, while cavities 3 and 4 have $R_j^{\rm in} = 0.9$ and $R_j^{\rm out} = 0.999$. The loss parameter of each cavity j is given by

$$\xi_j = \sqrt{R_j^{\rm in} R_j^{\rm out} e^{-2d_j\alpha_j}}, \tag{7}$$

where $\alpha_j = 0.35$ m^{-1}, while the average number of round trips for a photon in the cavity is given by $m_j = (1 - \xi_j)^{-1}$. The parameters adopted for the numerical simulation are, respectively, the set of coupling coefficients between the cavities of the network, the dissipation rate, and the transmission rate from site 2 to the output mode $\mathbf{k}_{\rm det}$ (i.e., the detector).

A. Dissipation rate

The dissipation rate in each cavity j can be evaluated by considering the amount of losses in m_j round trips, i.e., the average flight time of the photon in the cavity. Such a parameter can be evaluated according to the following expression:

$$\Gamma_j \sim \frac{D}{m_j t_j} \sum_{i=0}^{m_j} \xi_j^{2i} = D \frac{1 - \xi_j^{2(m_j+1)}}{(1 - \xi_j^2) m_j t_j}, \tag{8}$$

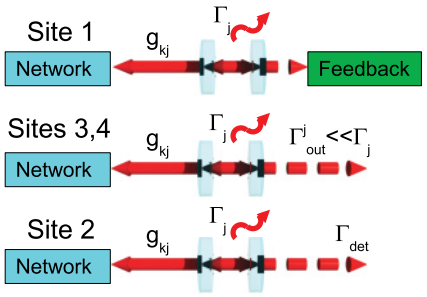

FIG. 3. (Color online) Scheme of all coupling, dissipation, and dephasing processes of the network. All sites are coupled with the network with g_{kj} couplings, and undergo both a dephasing process, with rate γ, and internal losses, with rate Γ_j. Site 1: external losses are reduced with a feedback system. Site 2: external coupling with the sink. Sites 3 and 4: external losses are negligible with respect to internal losses ($\Gamma^j_{\rm out} \ll \Gamma_j$).

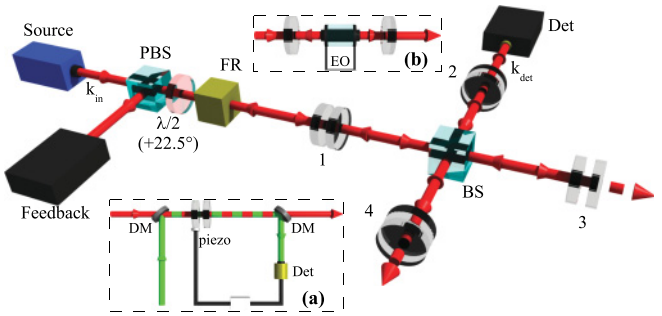

FIG. 4. (Color online) Experimental setup for the four-cavities optical network. The single photon in the input mode $\mathbf{k}_{\rm in}$ is injected into the network at site 1. The successful transfer of the excitation in the network is given by the detection of the single photon on mode $\mathbf{k}_{\rm det}$. The coupling coefficients between cavities can be changed by varying the transmittivity and the reflectivity of the beam-splitter (BS). The feedback system to reduce the dissipation rate $\Gamma^1_{\rm out}$ from site 1 exploits the polarization degree of freedom of the photon as described in the text. Inset (a): Sketch of an active phase stabilization apparatus. An auxiliary laser is injected and extracted into the network by two dichroic mirrors (DM). The measurement on the auxiliary laser is used to drive a piezoelectric system which stabilizes the cavity length. Inset (b): Introduction of dephasing rate by modulation of the index of refraction through an electro-optical crystal.

where ξ_j^2 represents the fraction of optical power which remains confined in the cavity after each round trip, t_j is the photon flight time in one round trip, m_j is the average number of round trips for the photon in cavity j, and D is the dissipation in one round trip only due to diffraction or coupling with other optical modes, i.e., $D = 1 - e^{-2\alpha_j d_j}$. Equation (8) evaluates the fraction of optical power lost in m_j round trips, divided by the average flight time $t_{\rm cav} = m_j t_j = 2dm_j/c$, with c being the speed of light. In our setup, one has $\Gamma_j \simeq 50$ MHz and $D \sim 0.007$. We consider the losses between the cavities and the beam-splitter to be negligible due to the adoption of antireflection coating optics. Notice that the average flight time of the photon in the cavity, i.e., $t_{\rm cav}$, is of the order of nanoseconds and defines the time scale of the process. Hence, the corresponding linewidth of the cavity alone, evaluated from the spectral properties of the intracavity field, is ~2 GHz. The linewidth of the injected photon must be much smaller than this value, hence a narrow-band parametric down-conversion source, such as one obtained through periodically poled nonlinear crystals, is necessary for an efficient cavity-photon coupling. Let us note that the presence of external mirrors with reflectivities $R^{\rm out}_{1,2,4} < 1$ introduces additive channels $\Gamma_{\rm out}$ for losing the photon from the network in spatial modes $\mathbf{k}^{\rm out}_{1,2,4}$—see Fig. 3. The dissipation rate due to such a process is given by the fraction of optical power lost through the external mirror in time $t_{\rm cav} = m_j t_j$, and can be evaluated as

$$\Gamma^j_{\rm out} \sim \frac{\left(1 - R^{\rm out}_j\right)}{m_j t_j} \sum_{i=0}^{m_j} \left(R^{\rm out}_j\right)^i = \frac{1 - \left(R^{\rm out}_j\right)^{m_j+1}}{m_j t_j} . \quad (9)$$

For cavities 3 and 4, such an additive dissipation channel is of the order of $\Gamma^{3,4}_{\rm out} \sim 10$ MHz, thus being negligible with respect to the dissipation due to intracavity losses. For cavity 1, we can introduce a feedback system to discard those events which correspond to losing the photon through this channel. This system is shown in Fig. 4 and exploits the polarization state of the photon by inserting a Faraday rotator (FR). More specifically, the photon with $|H\rangle$ polarization state, after the polarization beam-splitter (PBS), is rotated by the $\lambda/2$ waveplate and by the Faraday rotator in the polarization state $|V\rangle$. When the photon exits the network from the external mirror of site 1, propagation through the $\lambda/2$ waveplate and the Faraday rotator in the opposite direction maintains its polarization state $|V\rangle$ unaltered. Finally, the photon is reflected by the polarization beam-splitter and then detected. This allows us to discard those events when the detector clicks, thus reducing the effective dissipation term $\Gamma^1_{\rm out}$. We notice that recent papers have reported the realization of high detection efficiency (~75%) silicon avalanche photodiodes and superconducting transition edge detectors, with the perspective of reaching a value of $\eta_{\rm det} \sim 90\%$ [27,28]. The adoption of these devices would reduce the effective dissipation $\Gamma^1_{\rm out}$ due to the external mirror by a factor of 0.2, and hence in our case from ~100 MHz without post-selection to $\Gamma^1_{\rm out} \sim 20$ MHz.

B. Coupling rate

The cross-coupling coefficients have been evaluated following the theory of Marcuse [29,30]. The time evolution of the intracavity field amplitude is described by the following set of first-order differential equations:

$$\frac{dA^\nu_j}{dt} = i\left(\Omega^\nu_j - \Omega\right)A^\nu_j + i\sum_\sigma s^{\nu\sigma}_j A^\sigma_j + i\sum_{k\neq j}\sum_\sigma g^{\nu\sigma}_{jk} A^\sigma_k , \quad (10)$$

where j is the cavity index, (ν,σ) are the mode indices, $s^{\nu\sigma}_j$ and $g^{\nu\sigma}_{kj}$ are respectively the self-coupling and cross-coupling coefficients, Ω^ν_j is the optical frequency corresponding to the eigenvalue of the propagation equation for the optical mode ν in cavity j, Ω is a reference frequency corresponding to the center of the spectrum for Ω^ν_j, and A^ν_j are the field amplitudes. In our case, we consider only a single mode of the electromagnetic field, and the mode indexes (ν,σ) can be neglected. An approximate expression for the evaluation of the

cross-coupling coefficients is derived in Ref. [29] and reduces here to the expression

$$g_{kj} \simeq \frac{1}{2i}\left(\frac{v_k v_j}{d_k d_j}\right)^{1/2} t_{kj}, \tag{11}$$

where v_j are the intracavity group velocities, d_j are the cavity lengths, and t_{kj} is the amplitude transmission coefficient between the fields A_j and A_k in the two sites. The amplitude transmission coefficient can be directly evaluated by analyzing the fields in the classical limit. The calculation of this parameter can be divided into three intermediate steps. In the following we specify these calculations for our setup in Fig. 2.

1. *Output field from cavity k.* As a first step, we evaluate the ratio between the intracavity field and the field at the output of cavity k, given by

$$\frac{A_{\rm out}^{(k)}}{A_{\rm cav}^{(k)}} = \sqrt{\left(1-R_k^{\rm in}\right)}\left(e^{-i\delta\phi_k}e^{-\alpha_k d_k}\right), \tag{12}$$

where $\delta\phi_k$ is the phase term due to propagation inside cavity k.

2. *Intercavity field at the input face of cavity j.* The field at the input face of cavity j can be evaluated as the coherent superposition of all possible paths of the output field from site k, i.e., $A_{\rm out}^{(k)}$. Such a quantity strongly depends on interference effects between all possible paths that the photons can take in the network. We restrict our treatment only to the first-order path. The ratio between the intercavity field and the field at the output of cavity k, i.e., $I_{kj} = A_{\rm inter}^{(k\to j)}/A_{\rm out}^{(k)}$, has the following form:

$$I_{kj} = i^{n_r}\frac{1}{\sqrt{2}}e^{i(\phi_k+\phi_j)}K_{kj}, \tag{13}$$

where n_r is the number of times the photon has been reflected by the beam-splitter, $\phi_k = 2\pi\frac{l_k}{c}\nu_L$ is the phase shift due to spatial propagation between the cavity k and the BS, ν_L being the field optical frequency and l_k being the distance between the cavity k and the central BS; the form of K_{kj} is different depending on whether the cavities k and j are directly linked by the beam-splitter or not, i.e.,

$$K_{kj} = \begin{cases} 1 & \text{for direct link,} \\ \frac{1}{\sqrt{2}}\left(\sqrt{R_q^{\rm in}}e^{i2\phi_q} + \sqrt{R_p^{\rm in}}e^{i2\phi_p}\right) & \text{for indirect link,} \end{cases} \tag{14}$$

where p and q are cavity indices satisfying $k \neq j \neq p \neq q$. In order to generalize the expressions of I_{kj} and K_{kj} to the case of a BS with transmittivity $\eta \neq 0.5$, each factor $\frac{1}{\sqrt{2}}$ has to be replaced with $\sqrt{\eta}$ or $\sqrt{1-\eta}$ depending on whether the photon has been reflected or transmitted by the beam-splitter.

3. *Intracavity field in cavity j.* The intracavity field in site j is related to the intranetwork field at its input face according to

$$\frac{E_{\rm cav}^{(j)}}{E_{\rm intra}^{(k\to j)}} = \frac{\sqrt{\left(1-R_j^{\rm in}\right)}}{1-m_j}, \tag{15}$$

hence the coupling coefficients can be finally written as

$$g_{kj} = \frac{I_{kj}}{2i}\left(\frac{v_k v_j}{d_k d_j}\right)^{1/2}\frac{\sqrt{\left(1-R_k^{\rm in}\right)\left(1-R_j^{\rm in}\right)}e^{-i\delta\phi_k}}{1-m_j}e^{-\alpha_k d_k}. \tag{16}$$

Following these calculations, the absolute values of the coupling rates are found to be $g_{12} = 4.3$ GHz, $g_{13} = 5.7$ GHz, $g_{14} = 7.6$ GHz, $g_{23} = 6.1$ GHz, $g_{24} = 4.5$ GHz and $g_{34} = 5.9$ GHz. To take into account the fluctuations in the coupling coefficients (induced by the phase fluctuations) between experiments, we analyze also the case in which there is a static disorder of $\sim$20% in the coupling rates.

C. Transmission rate

Finally, the transmission rate from cavity 2 to the output mode $\mathbf{k}_{\rm out}$ is evaluated as above for Γ_j, by considering the amount of field which is transmitted through the mirror $R_2^{\rm out}$ in the output mode in m_2 round trips. In other words, the rate at which the photon is transferred to the detector can be evaluated with the same expression for the external mirror dissipation rate of Eq. (9). The numerical evaluation of this parameter gives

$$\Gamma_{\rm det} = \frac{1-\left(R_2^{\rm out}\right)^{m_2+1}}{m_2 2d/c} \sim 1\ \text{GHz}. \tag{17}$$

D. Experimental tasks

The two main challenges for the proposed experimental realization, shown in Fig. 4, regard the phase stability of the cavities and the implementation of a suitable device to introduce the necessary amount of dephasing rate. An accurate control on the cavity length is necessary in order to maintain the cavities at resonance with the photon wavelength and to keep the coupling rates constant. This phase stabilization can be achieved by an active feedback system working on an auxiliary laser superimposed with the single photon by means of a dichroic mirror, and then measured after its passage through the cavity [Fig. 4, inset (a)]. The parameters of this network correspond to a low-finesse optical cavity. Hence, a length stability of the order of few nanometers is necessary, which is a requirement fully achievable with the current technology.

The dephasing rate inside the cavity can be introduced by acting on the beam path, through the propagation factor e^{ikz}. This can be done by modifying the propagation length z or by varying the wave vector k, for instance by acting on the index of refraction inside cavity n. The phase modulation can then be achieved by different methods, depending on the desired modulation rate. For a dephasing rate of the order of 1 GHz, such as the one used in the numerical simulation in the following, an electro-optic or acousto-optic modulator can be inserted in the cavity to shift the frequency of light [Fig. 4, inset (b)].

IV. RESULTS OF THE NUMERICAL SIMULATION

In this section we investigate the dynamics of the optical cavity network by using our model with the coupling rates g_{ij} as estimated earlier, a dissipation rate set at $\Gamma_j = 70$ MHz for all the sites by taking into account the different dissipative processes, and a transfer rate to the detector of $\Gamma_{\rm det} = 1$ GHz. In particular, in Fig. 5 we show the cavity photonic population as a function of time in both cases of local dephasing (with rate 1 GHz) and no dephasing. The introduction of dephasing reduces the destructive interference between all the possible

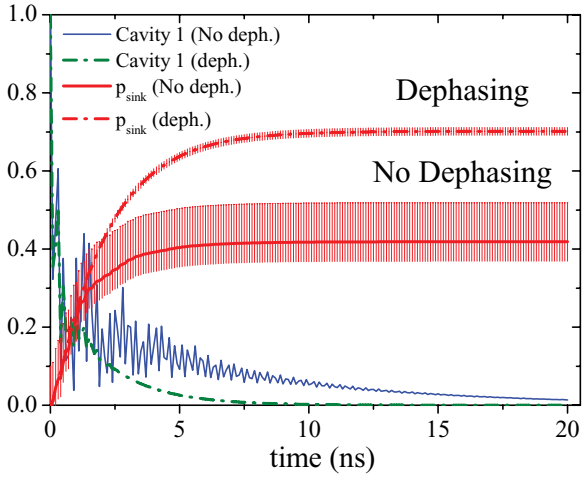

FIG. 5. (Color online) Site 1 population behavior and transfer efficiency vs time (in ns) for the optical cavity network for the noiseless (continuous line) and noisy (dashed line) case. The photon transmission is significantly enhanced by the presence of dephasing. The error bars are calculated considering a 20% static disorder (10^3 samples).

photon pathways and increases remarkably the overall transfer efficiency from about 40% to more than 70%. In the absence of dephasing, the photon is trapped in some superposition (dark) states which are not coupled to site 2, and this explains the lower transfer efficiency—see Ref. [10] for more details. Moreover, we consider also the case in which the coupling rates suffer a static disorder of 20% and plot the transfer efficiency as a function of the dephasing rate in Fig. 6. These results further support the prediction that noise-assisted transport could be experimentally observed by the present optical setup.

Finally, to quantify the entanglement dynamics, we study logarithmic negativity [31], i.e., $E(A|B) = \log_2 \|\rho^{\Gamma_A}\|_1$, measuring the entanglement across a bipartition $A|B$ of a composite system, where Γ_A is the partial transpose operation of the density operator ρ with respect to the subsystem A and $\|\cdot\|_1$ denotes the trace norm. In Refs. [10,11], in the context

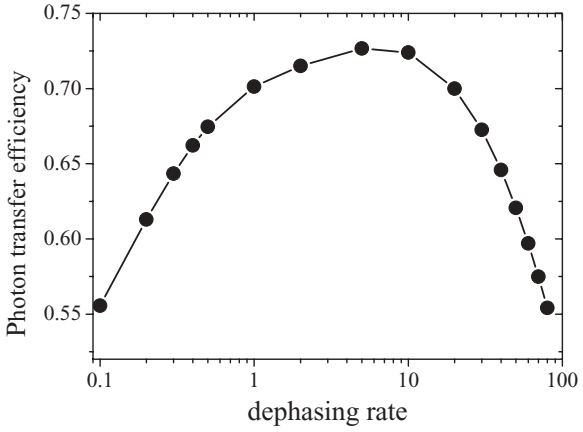

FIG. 6. Dependence of p_{sink} at a fixed time $t = 20$ ns as a function of the dephasing rate γ. These results show the remarkable robustness of this process, supporting the possibility that it could be experimentally observed.

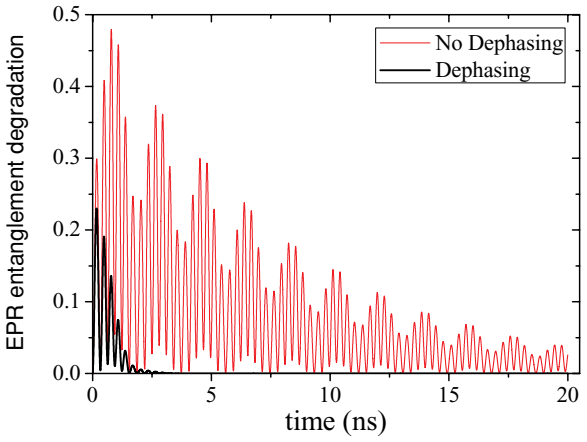

FIG. 7. (Color online) Degradation of entanglement between two photons (initially in a maximally entangled state), in which only one photon is sent to the network through cavity 1. It is measured in terms of log-negativity between the ancilla photon and the photon leaving cavity 2 (no detector).

of light-harvesting systems, it was found that the increase in the transfer efficiency is not strictly related to the presence of entanglement between the sites of the network, and a similar behavior has been found here. However, to further explore the capabilities of this optical cavity network as a conduit for not just energy (or classical information) but quantum information, we show in Fig. 7 how another form of entanglement (in this context more relevant, as it is measureable more directly) degrades through it. To that end, we introduce an ancillary photon, which initially shares a maximally entangled state with the single photon injected into optical cavity 1, i.e., in the EPR state $1/\sqrt{2}(|0\rangle_{\text{anc}}|0\rangle_1 + |1\rangle_{\text{anc}}|1\rangle_1)$, with $|0\rangle$ and $|1\rangle$ representing, respectively, the absence and presence of a photon [32,33]. As the system evolves, the entanglement between the ancillary photon and the photon leaving cavity 2 oscillates in time and almost vanishes in the presence of dephasing.

V. CONCLUSIONS AND OUTLOOK

We proposed a quantum optical network based on a set of coupled cavities, in order to investigate the effects of noise in excitation transfer. A detailed numerical simulation for experimentally realistic values shows the presence of a substantial enhancement in the photon transport efficiency when dephasing noise is introduced in the cavity. Finally, we note that a similar scheme can also be implemented by using a network of atoms in suitable ion traps [34]. The results reported here may open interesting perspectives for a deeper investigation of the fundamental mechanisms that underly the very highly efficient excitation transfer in light-harvesting complexes and for possible applications in solar-cell technology. Finally, this type of experiment can also trigger significant activity in two different areas, namely the modeling of complex environments via controlled interactions and the development of noise-assisted protocols for quantum communication [13].

ACKNOWLEDGMENTS

This work was supported by the projects AST 2009, HYTEQ (FIRB-MIUR), CORNER, HIP, Q-ESSENCE, and the Humboldt Foundation. F.C. was also supported by a Marie Curie Intra European Grant within the 7th European Community Framework Programme.

[1] W. H. Zurek, Rev. Mod. Phys. **75**, 715 (2003).
[2] M. B. Plenio and S. F. Huelga, Phys. Rev. Lett. **88**, 197901 (2002).
[3] L. Hartmann, W. Dür, and H.-J. Briegel, Phys. Rev. A **74**, 052304 (2006).
[4] H. Lee, Y.-C. Cheng, and G. R. Fleming, Science **316**, 1462 (2007).
[5] V. I. Prokhorenko, A. R. Holzwarth, F. R. Nowak, and T. J. Aartsma, J. Chem. Phys. B **106**, 9923 (2002).
[6] G. S. Engel, T. R. Calhoun, E. L. Read, T.-K. Ahn, T. Mančal, Y.-C. Cheng, R. E. Blankenship, and G. R. Fleming, Nature (London) **446**, 782 (2007).
[7] M. Mohseni, P. Rebentrost, S. Lloyd, and A. Aspuru-Guzik, J. Chem. Phys. **129**, 174106 (2008).
[8] M. B. Plenio and S. F. Huelga, New J. Phys. **10**, 113019 (2008).
[9] P. Rebentrost, M. Mohseni, I. Kassal, S. Lloyd, and A. Aspuru-Guzik, New J. Phys. **11**, 033003 (2009).
[10] F. Caruso, A. W. Chin, A. Datta, S. F. Huelga, and M. B. Plenio, J. Chem. Phys. **131**, 105106 (2009).
[11] F. Caruso, A. W. Chin, A. Datta, S. F. Huelga, and M. B. Plenio, Phys. Rev. A **81**, 062346 (2010).
[12] A. W. Chin, A. Datta, F. Caruso, S. F. Huelga, and M. B. Plenio, New J. Phys. **12**, 065002 (2010).
[13] F. Caruso, S. F. Huelga, and M. B. Plenio, Phys. Rev. Lett. **105**, 190501 (2010).
[14] M. J. Hartmann, F. G. S. L. Brandão, and M. B. Plenio, Nat. Phys. **2**, 849 (2006).
[15] D. G. Angelakis, M. F. Santos, and S. Bose, Phys. Rev. A **76**, 031805(R) (2007).
[16] A. D. Greentree, C. Tahan, J. H. Cole, and L. C. L. Hollenberg, Nat. Phys. **2**, 856 (2006).
[17] D. Bouwmeester, I. Marzoli, G. P. Karman, W. P. Schleich, and J. P. Woerdman, Phys. Rev. A **61**, 013410 (1999).
[18] P. L. Knight, E. Roldan, and J. E. Sipe, Phys. Rev. A **68**, 020301(R) (2003).
[19] B. Do, M. L. Stohler, S. Balasubramanian, D. S. Elliott, C. Eash, E. Fischbach, M. A. Fischbach, A. Mills, and B. Zwickl, J. Opt. Soc. Am. B **22**, 499 (2005).
[20] M. A. Broome, A. Fedrizzi, B. P. Lanyon, I. Kassa, A. Aspuru-Guzik, and A. G. White, Phys. Rev. Lett. **104**, 153602 (2010).
[21] A. Schreiber, K. N. Cassemiro, V. Potocek, A. Gábris, P. J. Mosley, E. Andersson, I. Jex, and Ch. Silberhorn, Phys. Rev. Lett. **104**, 050502 (2010).
[22] H. B. Perets, Y. Lahini, F. Pozzi, M. Sorel, R. Morandotti, and Y. Silberberg, Phys. Rev. Lett. **100**, 170506 (2008).
[23] D. N. Christodoulides, F. Lederer, and Y. Silberberg, Nature (London) **424**, 817 (2003).
[24] J. L. O'Brien, A. Furusawa, and J. Vuckovic, Nat. Photonics **3**, 687 (2009).
[25] A. Peruzzo *et al.*, Science **329**, 1500 (2010).
[26] E. Amselem, M. Radmark, M. Bourennane, and A. Cabello, Phys. Rev. Lett. **103**, 160405 (2009).
[27] O. Thomas, Z. L. Yuan, J. F. Dynes, A. W. Sharpe, and A. J. Shields, Appl. Phys. Lett. **97**, 031102 (2010).
[28] K. Tsujino, D. Fukuda, G. Fujii, S. Inoue, M. Fujiwara, M. Takeoka, and M. Sasaki, Opt. Express **18**, 8107 (2010).
[29] D. Marcuse, IEEE J. Quantum Electron. **21**, 1819 (1985).
[30] D. Marcuse, IEEE J. Quantum Electron. **22**, 223 (1986).
[31] M. B. Plenio and S. Virmani, Quant. Inf. Comp. **7**, 1 (2007).
[32] E. Lombardi, F. Sciarrino, S. Popescu, and F. De Martini, Phys. Rev. Lett. **88**, 070402 (2002).
[33] S. Giacomini, F. Sciarrino, E. Lombardi, and F. De Martini, Phys. Rev. A **66**, 030302(R) (2002).
[34] K. L. Brown, W. J. Munro, and V. M. Kendon, Entropy **12**, 2268 (2010).